Early hydration behavior of blended cementitious systems containing calcined clays and superplasticizer

Ricarda Sposito[1,a], Marlene Schmid[2,b], Nancy Beuntner[1,c], Sebastian Scherb[1,d], Johann Plank[2,e], Karl-Christian Thienel[1,f]

[1]*Institute for Construction Materials, University of the Bundeswehr Munich, Neubiberg, Germany*
[2]*Chair of Construction Chemistry, Technical University Munich, Garching, Germany*

[a]ricarda.sposito@unibw.de
[b]marlene.schmid@bauchemie.ch.tum.de
[c]nancy.beuntner@unibw.de
[d]sebastian.scherb@unibw.de
[e]sekretariat@bauchemie.ch.tum.de
[f]christian.thienel@unibw.de

ABSTRACT

Calcined clays represent a promising material because of worldwide deposits of suitable clays and low CO_2 emissions during calcination process for facing the increasing demand for sustainable supplementary cementitious materials (SCM). One side effect of calcined clays is their high water demand as compared to cements. The application of superplasticizers is inevitable to ensure the workability of concretes with calcined clays as SCM. Early hydration kinetics, namely silicate and aluminate reaction of clinker phases, can be significantly modified by superplasticizers. Until now, their compatibility was barely investigated although it depends mainly on type of superplasticizer and on mineralogy of calcined clays. Main objective of this study is to evaluate the influence of selected superplasticizers on reaction kinetics of blended cementitious systems containing different types of calcined clay by investigating their hydration behavior.

Four calcined clays are investigated: one calcined mixed layer clay which contains in its natural form approximately 25 w% kaolinite and 45 w% 2:1 clay minerals. The interaction with superplasticizers and those individual phyllosilicates is investigated on an industrially-used flash-calcined metakaolin, a calcined illitic clay and a calcined muscovite. Two different types of superplasticizers are used. One ordinary Portland cement and one Portland limestone cement are used as cement components.

The hydration kinetics of blended cement pastes is measured by isothermal calorimetry in combination with in-situ X-ray diffraction during first 48 hours of hydration at a temperature of 25 °C. The findings are completed by investigations with scanning electron microscopy at different timings during early hydration.

1. INTRODUCTION

Calcined clays as potential supplementary cementitious material (SCM) come strongly into focus of research (Antoni 2013, Beuntner 2017, Tironi et al. 2014). Especially calcined mixed layer clays with different phyllosilicates and further minerals are interesting as future SCM as they are available in sufficient quantities worldwide. Calcined clays have a pozzolanic impact on clinker reaction kinetics already during early hydration (Beuntner 2017, Danner et al. 2012, Scherb et al. 2018). Beside further CO_2 savings (Cancio Díaz et al. 2017), the addition of limestone is known to have good synergy effects with calcined clays in cementitious systems (Antoni et al. 2015, Martirena Hernández & Scrivener 2015, Tironi et al. 2017, Vance et al. 2013). The mineralogy of clay has according to Hermann & Rickert (2015) a significant impact on the specific surface area and hence on the required dosages of superplasticizers. Calcined clays exhibit a high specific surface area and water demand and require the use of superplasticizers in concrete (Thienel & Beuntner 2018).

There is a wide range of observations when it comes to the influence of superplasticizers on the hydration kinetics of ordinary Portland cement. According to Prince et al. (2002), polynaphthalene sulfonate superplasticizers retard the hydration of C_3A while Roncero et al. (2002) found out that both polycondensates and PCE polymers accelerate the reaction of C_3A, the formation of ettringite and the dissolution of gypsum. Sakai et al. (2006) also observed an accelerated reaction of C_3A but a lower rate of hydration due to the addition of different types of superplasticizers. These findings were also made by Lothenbach et al. (2007) investigating a PCE with OPC: the dissolution of C_3S was strongly retarded during the first 30 h of hydration by adding PCE. Investigations on the interaction of calcined clays and lignosulfonates revealed that dosages required for equal dispersion effects exceed dosage limits and lead to strong retardation effects (Sposito et al. 2018). Polycondensates retard the aluminate clinker reaction and formation of ettringite (Zaribaf & Kurtis 2018), but also accelerate pozzolanic reaction of metakaolin compared to PCE (Ahn et al. 2015). According to Ng & Justnes (2015) and Zaribaf & Kurtis (2018), PCE exhibit the highest dispersion effectiveness and the least influence on hydration kinetics. Taking this knowledge into account, the impact of diverse superplasticizers on the hydration behavior of cementitious systems blended with different types of cements and calcined clays is investigated.

2. MATERIALS AND METHODS

2.1 Materials

2.1.1 Cements

One ordinary Portland cement (OPC) CEM I 42.5 R and one Portland limestone cement (PLC) CEM II/A-LL 32.5 R, complying with (DIN EN 197-1 2011), are used. Their mineral phase contents are given in Table 1 and the physical parameters are listed in Table 3.

Table 1. Mineralogical analysis of cements (information provided by producer)

Cement	Mineral phase [wt%]						
	C_3S	C_2S	C_3A	C_4AF	CaO_{free}	Sulfates	Calcite
OPC	61.6	18.2	5.8	9.0	0.6	3.2	0.6
PLC	48.9	15.2	5.1	8.1	0.1	4.0	14.4

2.1.2 Calcined clays

Three calcined phyllosilicates and one calcined mixed layer clay are investigated. The metakaolin (Mk) is an industrially used product, flash-calcined at 550 °C with 93 wt% amorphous content, 5 wt% quartz and traces of anatase and mica. Metaillite (Mi) and metamuscovite (Mu) are calcined for 60 min in a lab muffle kiln at 770 °C (Mi) and 800 °C (Mu). The temperatures were chosen according to dehydroxylation temperature obtained by DTG and by highest solubility of Al- and Si-ions in alkaline solution. Mi possesses 56.4 wt% amorphous content, 4.9 wt% calcite, 38.2 wt% illite and traces of portlandite and lime. Mu has 19.2 wt% amorphous phases and 80.8 wt% muscovite (high-temperature modification). The origin, the calcination procedure and the grinding process of the mixed layer clay (TG) are described in (Beuntner & Thienel 2017, Gmür et al. 2016). Its mineralogical composition is given in Table 2, the

solubility of Al and Si ions of calcined clays and the physical parameters of all binders are displayed in Table 3.

Table 2. Mineralogical composition of calcined mixed layer clay (TG)

	Phase [wt%]										
	Quartz	Muscovite	Calcite	Illite	Chlorite	Feldspar	Secondary Silicates	Hematite	Ores	Sulfates	Amorphous
TG	16.2	2.2	0.6	4.6	0.4	6.0	6.3	0.6	1.1	1.6	60.8

Table 3. Physical parameters of cements (OPC, PLC), metakaolin (Mk), metamuscovite (Mu), metaillite (Mi) and calcined mixed layer clay (TG)

Parameter	Method	OPC	PLC	Mk	Mu	Mi	TG
Particle density [g/cm³]	He-pycnometer	3.17	3.09	2.61	2.79	2.72	2.63
Specific surface area [m²/g]	(DIN ISO 9277 2003)	1.0	1.7	17.8	11.8	94.6	3.9
Water demand [wt%]	(DIN EN 196-3 2009)	28.9	28.2	34.5	55.4	38.6	30.5
d_{10} [µm]	(ISO 13320 2009)	4.1	2.3	3.0	9.3	2.7	4.0
d_{50} [µm]		15.8	13.1	14.8	19.2	6.8	13.2
d_{90} [µm]		46.0	46.0	76.2	45.7	61.9	37.0
Si-ions solubility [wt%]	Inductively coupled plasma optical emission spectrometry (ICP-OES)	-	-	15.65	0.51	4.02	1.80
Al-ions solubility [wt%]		-	-	14.25	0.26	1.55	1.09
Si/Al ratio [-]		-	-	1.10	1.93	2.59	1.65

2.1.3 Superplasticizers

Two industrial superplasticizers are selected to investigate their influence on the hydration behavior on calcined clay blended cementitious systems. As representative for polycondensates, the calcium salt of a β-naphthalene sulfonate formaldehyde polycondensate (abbreviation: *NSF*) with a solid content of 40.0 wt% is used. As polycarboxylate-based superplasticizer, an α-methallyl-ω-methoxy poly(ethylene glycol) ether (HPEG) type PCE with a long side chain and a high anionic charge density (abbreviation: *HPEG*) is investigated. Its solid content is 50.0 wt%.

The dosages of superplasticizers (Table 4) are adjusted for each binder system in cement paste for a constant spread of 26 cm ± 0.5 cm by a modified mini slump test according to (DIN EN 1015-3 2007).

All dosages represent the active agent as % by weight of binder (%bwob) and are constantly used for all methods.

Table 4. Dosages of superplasticizers [%bwob]

Superplasticizer	OPC with					PLC with				
	-	20Mk	20Mu	20Mi	20TG	-	20Mk	20Mu	20Mi	20TG
NSF	0.21	0.68	1.50	0.95	0.40	0.24	0.77	1.50	0.97	0.50
HPEG	0.05	0.19	0.16	0.37	0.07	0.06	0.20	0.16	0.40	0.08

2.2 Methods

The cements are constantly substituted by 20 wt% of calcined clays at a water-to-binder (w/b) ratio of 0.50. The samples are designated as *cement_substitution rate and type of calcined clay_dosage and type of superplasticizer.* The hydration kinetics are determined by isothermal calorimetry with TAM Air (TA Instruments, Delaware/USA) and by in-situ X-ray diffraction (XRD) at 25 °C. The blended binder is homogenized for 30 seconds before the blended cement pastes are mixed for 60 seconds by hand for all methods. The samples are transferred into plastic ampoules for calorimetric measurements. The resulting heat flow is calculated to 1 g of cement [mW/g_{cement}]. For in-situ XRD, the blended cement pastes are transferred into flat metal crucibles and covered by a Kapton film to prevent drying up of the fresh paste. The hydration behavior is observed by an X-ray diffractometer Empyrean (PANalytical, Almelo/Netherlands) with PIXcel[1D] detector and Bragg-Brentano[HD] monochromator. Each measurement is in a range from 6 to 40 °2Θ and takes 15 min. The XRD sample holder is connected to a temperature-controlled device. The development of crystalline phases is illustrated by using isolines view of software Highscore Plus 4.7 (PANalytical, Almelo/Netherlands). The time-dependent appearance and disappearance of phases is determined by qualitative peak analysis of ettringite (hkl phase 110) (Goetz-Neunhoeffer & Neubauer 2005), AFm-Hc (006) (Runcevski et al. 2012), gypsum (020) (Schofield et al. 2000) and portlandite (001) (Busing & Levy 1957). The ettringite (110) is chosen as there are overlaying effects of ettringite (010) and the high temperature modification of muscovite (002) (Catti et al. 1989) in the systems with metamuscovite and superplasticizers.

3. RESULTS AND DISCUSSION

3.1 Influence of superplasticizers on reaction kinetics during the first 48 hours of hydration

A small peak after the maximum indicates the aluminate reaction (dissolution of C_3A and strong precipitation of ettringite according to Hesse et al. (2011)) for OPC (Figure 1) while PLC exhibits a dominant peak due to aluminate reaction (Figure 2). The addition of calcined clays has a significant influence on the reaction kinetics. OPC/PLC_20Mi yield the highest peak intensities after only 8.2 h. The acceleration is attributed to the fineness and high specific surface area of Mi (see Table 3). The high main peaks of OPC/PLC_20Mk result from the high solubility of Al and Si ions of Mk (Table 3). The high main peak intensities for Mk and Mi systems both may result from overlaying silicate and aluminate reactions as described by Beuntner (2017) for Mk. Systems with Mu exhibit accelerated silicate reactions compared to systems with cement only despite the low solubility of ions and the comparably coarse granulometry of Mu (Table 3). OPC/PLC_20Mu show up broader shoulders and lower aluminate peak intensities compared to Mi and Mk systems, indicating still a significant pozzolanic contribution of Mu to hydration kinetics. In a less distinctive manner, the addition of 20 wt% TG to OPC does also slightly accelerate the reaction kinetics until the aluminate shoulder is reached due to its fineness compared to OPC. This effect does not apply to PLC systems as PLC and TG have a more similar fineness (Table 3). While there is no significant peak detectable in the declining heat flow curve of OPC, OPC_20TG exhibits a broad shoulder at 23 h, which can be associated with the pozzolanic contribution of TG to aluminate reaction. The heat flow curves for PLC_20Mu, PLC_20TG and PLC are congruent during the first 10 h and differ later on in the appearance and intensity of the aluminate peak. Hence, a good synergy effect of PLC and 20 wt% TG can be confirmed. Scherb et al. (2018) attribute furthermore the decline of the main peak of systems with calcined clays and limestone to the formation of AFm hemicarboaluminate (AFm-Hc) phase.
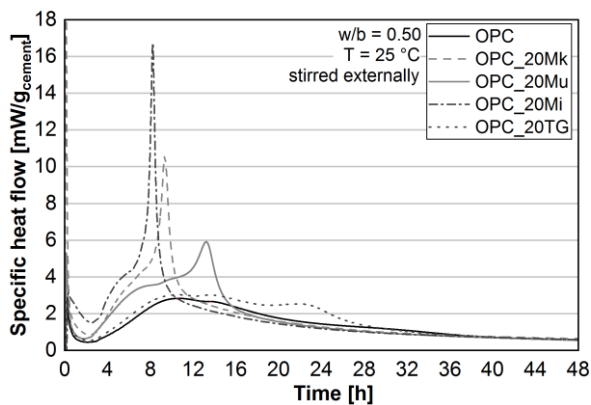
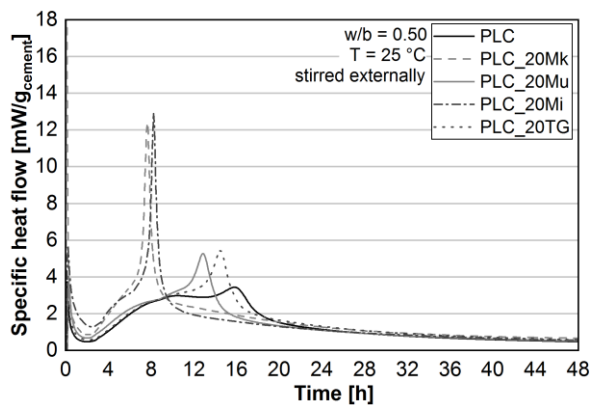**Figure 1. Heat flow of OPC systems without superplasticizers**

Figure 2. Heat flow of PLC systems without superplasticizers

Adding the polycondensate (NSF) has a retarding effect on the aluminate reaction by 1 h (OPC_0.21NSF/PLC_0.24NSF) which confirms findings of Prince et al. (2002). For systems with Mk, Mi or TG, the rest periods are prolonged by up to 1.7 h. Despite the high dosages of NSF in OPC_20Mi_0.95NSF and OPC_20Mk_0.68NSF and considering both the retarded end of rest period and occurrence of the aluminate peaks, the systems exhibit similar heat flow curves as OPC_20Mi/20Mk (Figure 3). The higher intensity of the main peak of OPC_20Mk_0.68NSF can be explained by overlapping chemo-mineralogical reactions and a boost of pozzolanic reactivity by polycondensates as already observed by Ahn et al. (2015). PLC_20Mi_0.97NSF shows up a general retardation of 1.5 h but a slightly higher intensity of the aluminate peak (Figure 4). Despite a lower dosage compared to PLC_20Mi_0.97NSF, PLC_20Mk_0.77NSF is more affected by NSF: the rest period is slightly more extended and the main peak is significantly less intense and occurs even 3.6 h later than without superplasticizer. Ten repeats of measurement were necessary for OPC/PLC_20Mu_1.50NSF due to bleeding during measurement. The averaging of the individual measurements shows a strong retardation of both the silicate and aluminate reaction. Although the systems with TG need the second lowest dosages of NSF, the superplasticizer has a certain influence on the reaction kinetics. Both systems are retarded by approximately 1 h compared to cement systems with NSF. Between 12 and 20 h, OPC_20TG_0.40NSF exhibits a constant level of heat flow, which is elevated afterwards by further pozzolanic contribution of TG. As the maximum peak is higher for OPC_20TG_0.40NSF (Figure 3) and occurs slightly earlier compared to OPC_20TG (Figure 1) without superplasticizer, NSF might provide a little boost to pozzolanic reactivity at least in systems with ordinary Portland cement. The findings of Ahn et al. (2015) on the interaction of metakaolin and polycondensates hence are also applicable to the investigated calcined mixed layer clay with OPC. Similar findings hold less pronounced also for PLC_20TG_0.50NSF (Figure 4) compared to PLC_20TG (Figure 2).
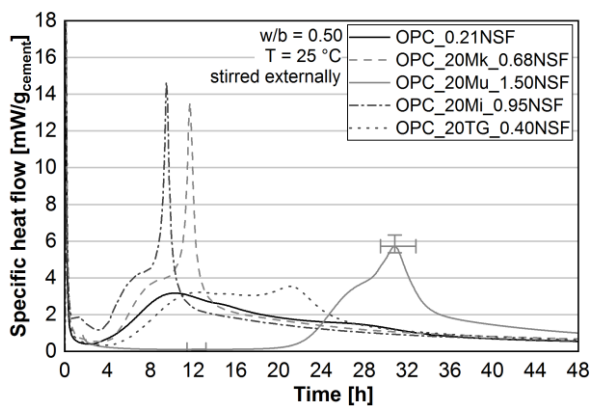

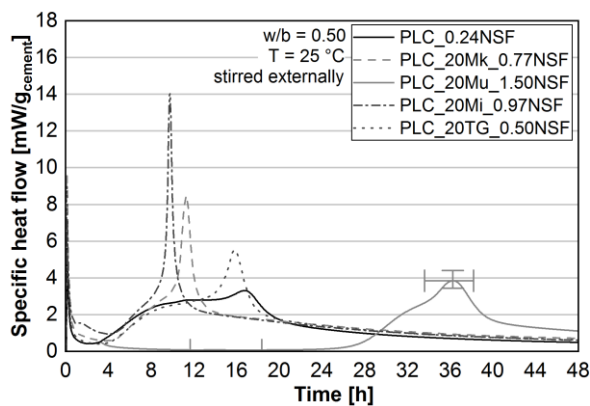**Figure 3. Heat flow of OPC_x_NSF systems**

Figure 4. Heat flow of PLC_x_NSF systems

Using HPEG superplasticizer leads to a slightly prolonged rest period for OPC_0.05HPEG (Figure 5) and PLC_0.06HPEG (Figure 6). For pure cement systems, the retarding effect of HPEG on aluminate

reaction is also less than the impact of NSF confirming earlier findings (Ng & Justnes 2015, Zaribaf & Kurtis 2018). The rest periods are shorter for all systems with calcined clays when HPEG is used instead of NSF. OPC_20Mk_0.19HPEG and OPC_20Mi_0.37HPEG exhibit lower main peak intensities at similar times compared to systems with NSF. This effect goes along with broader shoulders on the left side of the peaks, which indicate earlier ongoing hydration processes (Figure 5). Although PLC_20Mi_0.40HPEG has the highest dosage of HPEG, the retardation of the main peak compared to PLC_20Mi is negligible whereas PLC_20Mk_0.20HPEG exhibits a retardation of 1.3 h compared to PLC_20Mk with half the amount of HPEG used. OPC_20Mu shows up only a slight retardation of main peak whereas the HPEG PCE even has an immense acceleration effect on reaction kinetics in PLC_20Mu_0.16HPEG, both resulting in significantly higher intensities compared to OPC/PLC_20Mu. At low dosages (0.16 %bwob) of HPEG, they exhibit better compatibilities than with 1.50 %bwob NSF. Systems with TG and HPEG reveal similar heat flow curves as systems with OPC only and especially with PLC only: the curves of OPC_0.05HPEG and OPC_20TG_0.07HPEG are congruent during the first 14 h until the aluminate part of the pozzolanic reaction of TG commences. Compared to the systems without superplasticizer and with NSF, the curves of the PLC_20TG_0.08HPEG and the PLC_0.06HPEG system almost coincide and differ only in the intensity of their main peaks.
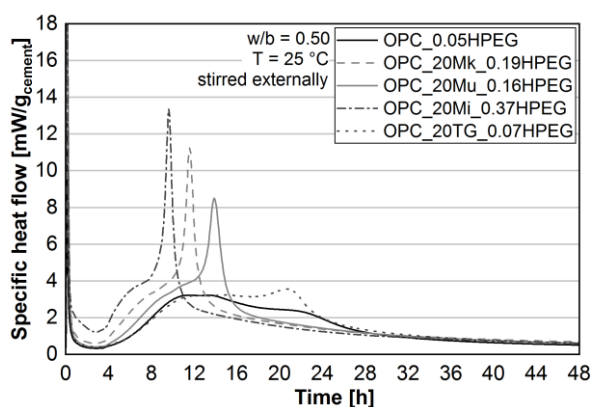
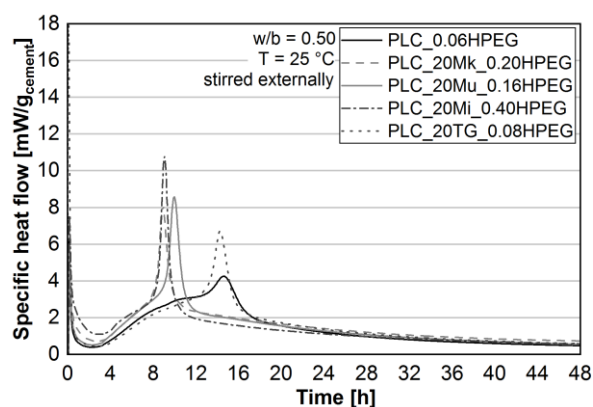

Figure 5. Heat flow of OPC_x_HPEG systems   **Figure 6. Heat flow of PLC_x_HPEG systems**

3.2 Influence of superplasticizers on formation of hydrate phases using the example of OPC and OPC-metamuscovite systems

Results from in situ XRD are limited to OPC and OPC_20Mu systems as the latter are influenced the most by superplasticizers. All systems show up an immediate formation of ettringite. It goes along with dissolution of gypsum, which is completed earlier for OPC_0.21NSF and later for OPC_0.05HPEG compared to OPC (Figure 7). The latter finding fits with results from Jansen et al. (2012) where a PCE retarded the dissolution of gypsum. While there is no formation of AFm-Hc during the first 48 h of hydration in the OPC system, both superplasticizers precipitate the formation of AFm-Hc, which is detectable after 28 h (OPC_0.21NSF) and 36.5 h (OPC_0.05HPEG). The formation of portlandite (CH) starts between 4.5 and 5 h for all OPC systems. The main part of CH formation is completed after 10 h (OPC_0.21NSF) and 11.5 h (OPC) while it persists until 16.5 h for OPC_0.05HPEG. These results fit well with the maxima in the heat flow curves from calorimetric measurements.

Gypsum is dissolved in OPC_20Mu earlier than in OPC as observed beforehand by Scherb et al. (2018). The dissolution of gypsum is accelerated further in OPC_20Mu_0.16HPEG (Figure 8) which explains the high intensity of its main peak in the heat flow curve in Figure 5. In OPC_20Mu_1.50NSF it takes 24.5 h to dissolve the gypsum completely. Formation of AFm-Hc starts after 20 h (OPC_20Mu) and 15 h (OPC_20Mu_0.16HPEG), while there is no AFm-Hc detectable in OPC_20Mu_1.50NSF during the first 48 h. Portlandite (CH) is detectable after 3.25 h (OPC_20Mu) and 4.75 h (OPC_20Mu_0.16HPEG) and the main reaction takes place until 13.5 and 12.5 h respectively. In OPC_20Mu_1.50NSF, the (main) formation of CH is strongly retarded. It does not start before a time of 12.5 h (Figure 8) and continues until 26.5 h. These observations confirm the results of isothermal calorimetry where the rest period of OPC_20Mu_1.50NSF does not end before a time of 12.5 h (Figure 3). Not least due to its extremely high amount, NSF retards both aluminate and silicate reaction in the cement-Mu system. HPEG promotes the aluminate reaction and slightly retards the silicate reaction. Winnefeld (2012) reports both a stronger retardation with increasing amount of superplasticizer and a stronger retardation of PCE than

of naphthalene sulfonate superplasticizers if the same amount is used. As less HPEG is needed for the same dispersion effects, it concludes that the retardation is less as well.
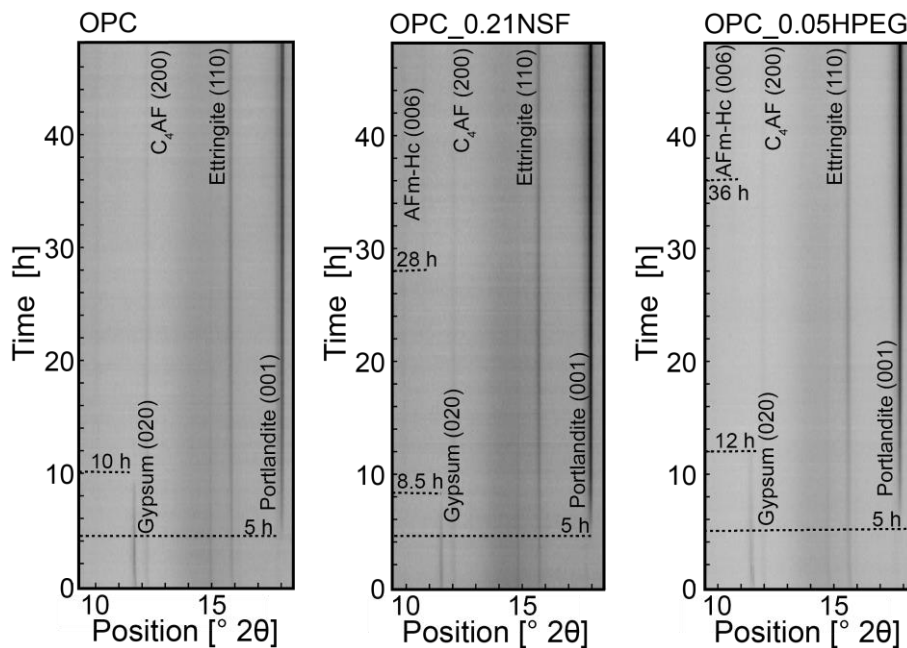

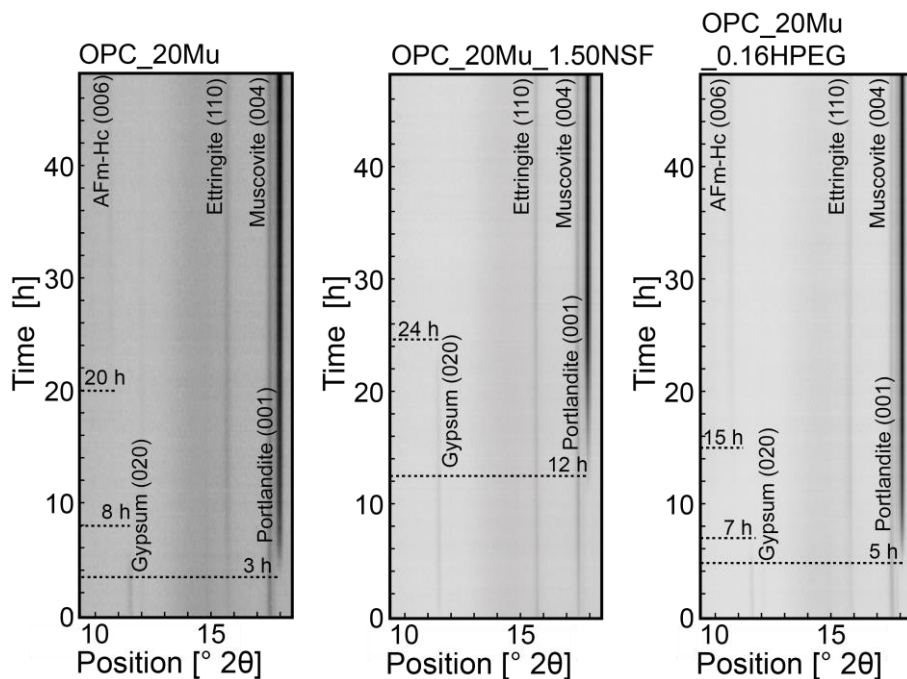**Figure 7. In situ X-ray plots from 9.5 to 18.5 °2Θ for OPC systems**

Figure 8. In situ X-ray plots from 9.5 to 18.5 °2Θ for OPC_20Mu systems

4. CONCLUSION

The previous investigation program highlights the effect of superplasticizers on the hydration kinetics of cementitious systems containing calcined clays. The main influences are on the dissolution of gypsum as sulfate carrier as well as on the beginning of formation of portlandite and AFm-Hc. Investigated binder systems require in general higher dosages of polycondensate than of PCE, which lead partially to stronger retardation effects. Selected systems exhibit incompatibilities with NSF indicated by late formation of portlandite or dissolution of gypsum whereas the investigated HPEG PCE exhibits a

superior compatibility with calcined clay blended cementitious systems and has only minor or partially even boosting impact on the pozzolanic reaction kinetics, e.g. on the formation of AFm-Hc. Nonetheless also the addition of NSF can slightly accelerate hydration kinetics confirming earlier findings from literature. Commonly known synergy effects between Portland limestone cement and calcined clays hold also for systems dispersed with superplasticizers.

Calcined mixed layer clays are particularly promising due to their mineralogical composition as they are capable to interact even with low dosages of superplasticizers thus resulting in good dispersing effects and exhibiting a similar hydration behavior as pure cement systems. In general, the influence of the amount of superplasticizer on the retardation of hydration increases non-linearly with increasing dosage and is compensated by the addition of calcined clays. In further studies, the demand for superplasticizers and the compensation of retarding effects by calcined clays should be considered in detail as there are - beside the mineralogy of calcined clays - several more parameters (e.g. grinding fineness) which affect the hydration kinetics.

5. ACKNOWLEDGEMENT

6. REFERENCES

Ahn, T-H, Shim, K-B, & Ryou, J-S (2015). „*The relationship between various superplasticizers and hydration of mortar incorporating metakaolin*," Journal of Ceramic Processing Research, Vol. 16, No. 2, pp. 181-187.

Antoni, M (2013). „*Investigation of cement substitution by blends of calcined clays and limestone*," Faculté des Sciences et Techniques de L'ingénieur, École Polytechnique Fédérale de Lausanne, Lausanne, 254 pp.

Antoni, M, Baquerizo, L, & Matschei, T (2015). „*Investigation of ternary mixes made of clinker limestone and slag or metakaolin: Importance of reactive alumina and silica content*," in *Calcined Clays for Sustainable Concrete*, Scrivener, K., and Favier, A., Editors. Springer Netherlands, pp. 545-553.

Beuntner, N (2017). „*Zur Eignung und Wirkungsweise calcinierter Tone als reaktive Bindemittelkomponente in Zement*," Fakultät für Bauingenieurwesen und Umwelt-wissenschaften, Universität der Bundeswehr München, Neubiberg, 207 pp.

Beuntner, N, & Thienel, K-C (2017). „*Performance and properties of concrete made with calcined clays*," in *ACI SP 320 - 10th ACI/RILEM International Conference on Cementitious Materials and Alternative Binders for Sustainabe Concrete*, Tagnit-Hamou, A., Editor. Sheridan Books, Montreal, Canada, pp. 7.1-7.12.

Busing, WR, & Levy, HA (1957). „*Neutron Diffraction Study of Calcium Hydroxide*," The Journal of Chemical Physics, Vol. 26, No. 3, pp. 563-568.

Cancio Díaz, Y, Sánchez Berriel, S, Heierli, U, Favier, AR, Sánchez Machado, IR, Scrivener, KL, Martirena Hernández, JF, & Habert, G (2017). „*Limestone calcined clay cement as a low-carbon solution to meet expanding cement demand in emerging economies*," Development Engineering, Vol. 2, pp. 82-91.

Catti, M, Ferraris, G, & G., I (1989). „*Thermal strain analysis in the crystal structure of muscovite at 700 °C*," European Journal of Mineralogy, Vol. 1, No. 5, pp. 625-632.

Danner, T, Ostnor, T, & Justnes, H (2012). „*Calcined marl as a pozzolan for sustainable development of the cement and concrete industry*,“ in ACI SP 289 - 12th International Conference on Recent Advances in Concrete Technology and Sustainability Issues. Prague, pp. 357-368.

DIN EN 196-3 (2009). „*Prüfverfahren für Zement - Teil 3: Bestimmung der Erstarrungszeiten und der Raumbeständigkeit (Methods of testing cement - Part 3: Determination of setting times and soundness)*“.

DIN EN 197-1 (2011). „*Zement - Teil 1: Zusammensetzung, Anforderungen und Konformitätskriterien von Normalzement (Cement - Part 1: Composition, specifications and conformity criteria for common cements)*“.

DIN EN 1015-3 (2007). „*Prüfverfahren für Mörtel für Mauerwerk-Teil 3: Bestimmung der Konsistenz von Frischmörtel (mit Ausbreittisch) (Methods of test for mortar for masonry - Part 3: Determination of consistence of fresh mortar (by flow table))*“.

DIN ISO 9277 (2003). „*Bestimmung der spezifischen Oberfläche von Feststoffen durch Gasadsorption nach dem BET-Verfahren (Determination of the specific surface area of solids by gas adsorption - BET method)*“.

Gmür, R, Thienel, K-C, & Beuntner, N (2016). „*Influence of aging conditions upon the properties of calcined clay and its performance as supplementary cementitious material*,“ Cement and Concrete Composites, Vol. 72, pp. 114-124.

Goetz-Neunhoeffer, F, & Neubauer, J (2005). „*Refined ettringite (Ca6Al2(SO4)3(OH)12·26H2O) structure for quantitative X-ray diffraction analysis*,“ Powder Diffraction, Vol. 21, No. 1, pp. 4-11.

Herrmann, J, & Rickert, J (2015). „*Interactions between cements with calcined clay and superplasticizers*,“ in 11th Int. Conference on Superplasticizers and Other Chemical Admixtures in Concrete. Ottawa, Canada, pp. 299-314.

Hesse, C, Goetz-Neunhoeffer, F, & Neubauer, J (2011). „*A new approach in quantitative in-situ XRD of cement pastes: Correlation of heat flow curves with early hydration reactions*,“ Cement and Concrete Research, Vol. 41, No. 1, pp. 123-128.

ISO 13320 (2009). „*Particle size analysis - Laser diffraction methods*“.

Jansen, D, Neubauer, J, Goetz-Neunhoeffer, F, Haerzschel, R, & Hergeth, WD (2012). „*Change in reaction kinetics of a Portland cement caused by a superplasticizer — Calculation of heat flow curves from XRD data*,“ Cement and Concrete Research, Vol. 42, No. 2, pp. 327-332.

Lothenbach, B, Winnefeld, F, & Figi, R (2007). „*The influence of superplasticizers on the hydration of Portland cement*,“ in *12th International Congress on the Chemistry of Cement*, Montreal, Canada pp.

Martirena Hernández, F, & Scrivener, K (2015). „*Development and introduction of a low clinker, low carbon, ternary blend cement in Cuba*,“ in *Calcined Clays for Sustainable Concrete*, Scrivener, K., and Favier, A., Editors. Springer, Dordrecht, pp. 323-329.

Ng, S, & Justnes, H (2015). „*Influence of dispersing agents on the rheology and early heat of hydration of blended cements with high loading of calcined marl*,“ Cement and Concrete Composites, Vol. 60, pp. 123-134.

Prince, W, Edwards-Lajnef, M, & Aïtcin, PC (2002). „*Interaction between ettringite and a polynaphthalene sulfonate superplasticizer in a cementitious paste*,“ Cement and Concrete Research, Vol. 32, No. 1, pp. 79-85.

Roncero, J, Valls, S, & Gettu, R (2002). „*Study of the influence of superplasticizers on the hydration of cement paste using nuclear magnetic resonance and X-ray diffraction techniques*,“ Cement and Concrete Research, Vol. 32, No. 1, pp. 103-108.

Runcevski, T, Dinnebier, RE, Magdysyuk, OV, & Pollmann, H (2012). „*Crystal structures of calcium hemicarboaluminate and carbonated calcium hemicarboaluminate from synchrotron powder diffraction data*,“ Acta Crystallographica Section B, Vol. 68, No. 5, pp. 493-500.

Sakai, E, Kasuga, T, Sugiyama, T, Asaga, K, & Daimon, M (2006). „*Influence of superplasticizers on the hydration of cement and the pore structure of hardened cement*,“ Cement and Concrete Research, Vol. 36, No. 11, pp. 2049-2053.

Scherb, S, Beuntner, N, Köberl, M, & Thienel, K-C (2018). „*The early hydration of cement with the addition of calcined clay - from single phyllosilicate to clay mixture*,“ in 20th International Conference on Building Materials. Weimar, Germany, pp. 658-666.

Schofield, PF, Wilson, CC, Knight, KS, & Stretton, IC (2000). „*Temperature related structural variation of the hydrous components in gypsum*,“ Zeitschrift für Kristallographie - Crystalline Materials, Vol. 215, No. 12, pp. 707.

Sposito, R, Dürr, I, & Thienel, K-C (2018). „*Lignosulfonates in cementitious systems blended with calcined clays*,“ in *SP-326 Durability and Sustainability of Concrete Structures - 2nd Workshop Proceedings*, Falikman, V., et al., Editors. Sheridan Books, Moscow, Russia, pp. 10.1-10.10.

Thienel, K-C, & Beuntner, N (2018). „*Calcinierte Tone und ihr Potenzial für die moderne Betontechnologie*,“ in 14. Symposium Baustoffe und Bauwerkserhaltung KIT - Betone der Zukunft - Herausforderungen und Chancen. Karlsruhe, pp. 37-48.

Tironi, A, Scian, AN, & Irassar, EF (2017). „*Blended cements with limestone filler and kaolinitic calcined clay: filler and pozzolanic effects*,“ Journal of Materials in Civil Engineering, Vol. 29, No. 9, pp. 8.

Tironi, A, Trezza, MA, Scian, AN, & Irassar, EF (2014). „*Potential use of Argentine kaolinitic clays as pozzolanic material*,“ Applied Clay Science, Vol. 101, pp. 468-476.

Vance, K, Aguayo, M, Oey, T, Sant, G, & Neithalath, N (2013). „*Hydration and strength development in ternary portland cement blends containing limestone and fly ash or metakaolin*,“ Cement and Concrete Composites, Vol. 39, pp. 93-103.

Winnefeld, F (2012). „*Interaction of superplasticizers with calcium sulfoaluminate cements*,“ in 10th International Conference on Superplasticizers and Other Chemical Admixtures in Concrete. Prague, pp. 17.

Zaribaf, BH, & Kurtis, KE (2018). „*Admixture compatibility in metakaolin–portland-limestone cement blends*,“ Materials and Structures, Vol. 51, No. 1, pp. 13.